EURASIAN PHYSICAL TECHNICAL JOURNAL

2025, Volume 22, No. 4 (54)

https://doi.org/10.31489/2025N4/31-38

Received: 23/06/2025 Revised: 14/11/2025 Accepted: 22/12/2025 Published online: 29/12/2025

Research Article

UDC 539.213.32

MODELING OF CLOSE-ORDER FRACTAL STRUCTURES OF METAL-METALLOID ALLOYS WITH CUBIC STRUCTURE

Sereda D.B., Baskevych O.S., Sereda B.P., Kryhliyak I.V.

[1] Dnipro State Technical University, Kamenskoe, Ukraine

[2] Ukrainian State University of Science and Technology, Dnipro, Ukraine

*Corresponding author: seredabp@ukr.net

Abstract. *Using methods of mathematical physics, a comprehensive simulation of the short-range order in $Fe_{88}P_{12}$ and $Cr_{88}C_{12}$ alloys produced by electrodeposition was carried out. As the initial configuration for modeling, the crystal structure of the base metal was selected. Numerous experimental studies, including X-ray diffraction and electron microscopy analyses, have indicated that in metal-metalloid alloys, surface microstructures predominantly exhibit ellipsoidal morphologies. Based on these experimental observations, it was hypothesized that the macroscopic ellipsoidal formations observed on the alloy surfaces are composed of clusters with relatively simple geometric configurations, such as spheres or ellipsoids. The results of the simulation revealed that these clusters possess characteristic sizes not exceeding 30-50 angstroms, and their vectorial growth predominantly occurs along a single radial direction relative to the substrate surface. This anisotropic growth behavior is attributed to differences in local atomic bonding energy and diffusion kinetics, which drive the preferential alignment of cluster development. Moreover, it was established that the spatial distribution and size uniformity of the clusters significantly influence the overall mechanical and physicochemical properties of the coatings, including hardness, wear resistance, and corrosion stability. The combination of modeling outcomes with empirical data provides valuable insight into the microstructural evolution mechanisms governing electrodeposited metal-metalloid systems. These findings can serve as a basis for optimizing the electrodeposition parameters to tailor the surface structure and enhance the performance characteristics of functional coatings.*

Keywords: amorphous state, electrodeposition, modeling, clusters.

1. Introduction

Amorphous and nanocrystalline metal alloys obtained by electrodeposition have a set of unusual physical and chemical properties and are a new class of promising materials of undoubted theoretical and practical interest. The structural state of metallic amorphous and nanocrystalline alloys is characterized by close atomic order and, unlike crystals, by the absence of translational symmetry in the arrangement of atoms. All amorphous materials have a short-range order, which is also called topological (or configurational), and the ordered distribution of different kinds of atoms is called the chemical (compositional) short-range order. Since it is problematic to obtain pure metals in an amorphous state, metalloid atoms are introduced to produce them. In the case of two- and multi-component systems, the concept of "near order" includes the spatial distribution of atoms regardless of the grade and mutual distribution of different-grade atoms [1-3]. The creation of promising and improvement of existing metal alloys for protective coatings using electrolytic deposition is impossible without establishing the mechanism of their formation and growth. Currently, there is no single theory of deposition of metal alloys depending on the conditions of their formation, which leads to great difficulties in interpreting the properties of these materials. Numerous experiments on the electrodeposition of

metal alloys show that the surface structures have different geometric shapes: two-dimensional surface shapes, and in some cases, three-dimensional (three-dimensional) shapes. It is known that one of the most important properties of the surfaces of fractal systems is the self-similarity property. If you select a small area in the surface area occupied by a fractal cluster, the cluster areas will be similar to the shape of this cluster. For clusters with random arrangements of atoms, it is necessary to use statistical particle sizes. During electrodeposition, the growth of such clusters is observed mainly in the direction opposite to the movement of metal ions and amorphizing elements [4-6]. The research of deposited metal pyrites with body-centered cube grill (BCC) showed that the surfaces have ellipsoidal forms of fractal structure and can be studied by means of fractal geometry, X-ray diffraction analysis and electron microscopy (Fig. 1-3). It has been found that the shape that the surface takes during crystallization is very sensitive to the crystallization conditions, and therefore it is impossible to establish the mechanism of surface growth from the growth of bulk forms. During electrodeposition, an atomic deposition occurs, which forms clusters with different shapes that depend on the orientation of the faces and the conditions of their growth in a certain direction. Surface fractal structures influence various physical objects and phenomena, in particular, to explain the corrosion resistance and wear resistance from the surface shape.

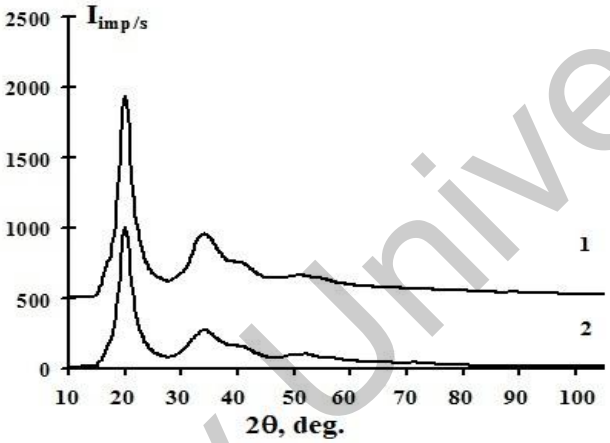

Fig. 1. X-ray diffractogram of $Cr_{88}C_{12}$ (1) and $Fe_{88}P_{12}$ (2) Mo-K_α radiation.

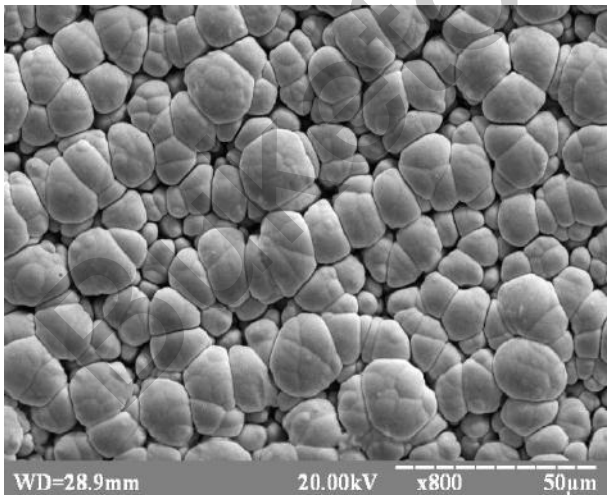

Fig.2. Surface morphology of $Cr_{88}C_{12}$ alloy (REMMA-102-2)

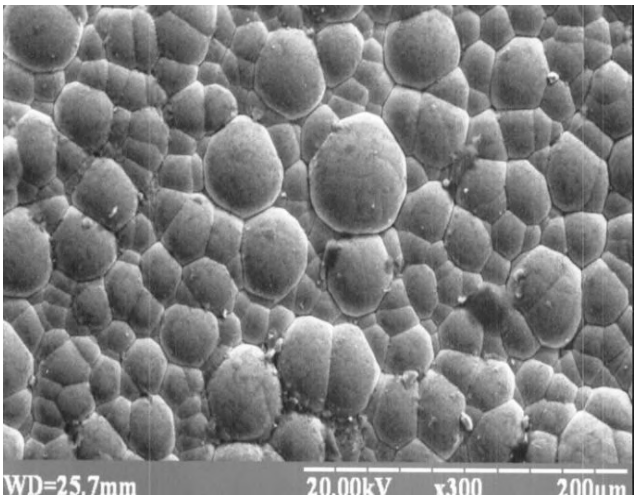

Fig.3. Surface morphology of $Fe_{88}P_{12}$ alloy (REMMA-102-2)

2. Material and methods of research

$Cr_{88}C_{12}$ alloys were obtained from an electrolyte of the following composition: $KCr(SO_4)_2 \cdot 12H_2O$ — 0.5 M, K_2BO_3 — 0.5 M, $(NH_4)_2SO_4$ — 2 M, HCOOH — 0.75 M, with pH adjusted to 3.0 and a temperature of 298 K. $Fe_{88}P_{12}$ alloys were obtained from an electrolyte of the following composition (in g/L): $FeSO_4 \cdot 7H_2O$ — 280, H_3BO_3 — 30, NaH_2PO_2 — 8×12. The pH was adjusted to 2.0–2.5 by the addition of a 5% H_2SO_4 solution. Deposition was performed using a unipolar pulsed current (i = 15–25 A/dm²) with a pulse repetition rate (f = 2–16 Hz) and a pulse duty cycle (Q = 2–4).

The identification of crystalline phases was carried out using X-ray diffractometry. X-ray diffractograms were obtained on a DRON-3.0 diffractometer with monochromatic Mo-Kα radiation (using a curved LiF monochromator) at measurement points with an interval of 0.1 degrees and an exposure time of less than 100 seconds per point, followed by averaging across five scattering intensity curves.

The quantitative composition and surface morphology were investigated using a REMMA-102-2 scanning electron microscope (SELMI), and the coating thickness was measured using a NU-2 optical microscope (Carl Zeiss).

3. Results and discussion

Numerous experiments on the electrodeposition of alloys with volume-centered cubic lattices have shown that ellipsoidal fractal forms grow (figs. 2 and 3). To establish the mechanism of fractal growth and their structure, we will use the Brave-Donneuil-Harker rule, which states that the crystal habitus is formed with the simplest plane indices, or the faces with the highest reticular atomic density have the lowest energy. For the case of materials with the OCC structure, the bounding planes are the (110) and (200) faces. When deposition by electric current occurs in the direction opposite to the action of the electric current, the deposition process has one growth vector, and other growth directions are of secondary importance. Consider the growth of a fractal structure in terms of the crystal structure of the base metal. As a result of deposition, crystallization centers appear on the substrate, which determine the further growth of clusters. As a result, additional crystallization centers appear on the formed clusters, which again form clusters of a similar shape. The shapes of the clusters and their close order can be determined by modeling the main peak of the structural factor. Since in this case, the deposition of Cr-C and Fe-P alloys has an amorphous structure (Fig. 1), it is necessary to determine their close order and the most likely cluster shape.

It is well known that during the formation of nanocrystalline and amorphous alloys, changes in their physical and chemical properties are observed. This always happens when approaching a certain critical size. The research of the close order of amorphous and nanocrystalline Cr-C and Fe-P alloys with a volume-centered cubic lattice structure allows us to establish the stability and sequence of crystallization processes. To determine the close order of amorphous Cr-C and Fe-P alloys, a methodology for its modeling based on the profile of the main peak of the structural factor is proposed. The profile of the main peak of the structural factor was approximated using the model of the cluster structure of the amorphous state. According to the chosen model, the expression for the diffraction peak profile takes into account the finiteness of the ordering regions, their size distribution, and the relative rms displacements of atoms from the equilibrium position and is defined by eq. [7-12]:

$$i(s_0) = \frac{Q_2 Q_3}{d_{hk}} \exp\left(-\frac{u^2 s_0^2}{2}\right) \int_{-\infty}^{\infty} V(t) \cdot g(L,t) \cdot e^{-\gamma(t)} \cos(s_0 t) dt, \quad (1)$$

where Q_2 and Q_3- coefficients that take into account the effect of relative rms displacements of atoms from equilibrium positions ($\bar{u}^2$) within the reflection plane on the height of the main peak of the structural factor, g(L, t) - distribution of clusters by size, L- size of clusters, V(t)- unction of shape, γ - coefficient, which determines the effect of the relative root mean square static displacements of atoms in the direction perpendicular to the reflection plane (during isothermal annealing $\gamma \to 0$), t - normal to a number of atomic planes that reflect radiation within the investigated diffraction peak, $s_0 = |s - s_{\max}|$- modulus of the scattering vector.

The function $V(\vec{t})$ is defined by the expression [9-11, 14]:

$$V(\vec{t}) = V^{-1} \int \sigma(\vec{x}) \sigma(\vec{x} + \vec{t}) d^3\vec{x}\,, \quad (2)$$

where V is volume of the cluster, and the function:

$$\sigma(\vec{x}) = \begin{cases} 1, x \in V \\ 0, x \notin V \end{cases}, \quad (3)$$

If the scattering region has ν planar grids perpendicular to the primary beam, then the intensity of the structural factor in the primary beam region (2) is converted to:

$$i(0) = \text{const}\left(1 + 2\sum_{p=1}^{v}\left(1 - \frac{p}{v}\right)\right) = \text{const} \cdot v, \quad (4)$$

For the scattering regions of disordered systems, the height of the main peak of the structural factor will be lower than that of crystalline and volume-centered cubic lattice nanalloys, and their height will be proportional to the size of this region. The coefficients Q_i for the volume-centered cubic lattice structure are equal Q_2 =0,9881 i Q_3=0,9766 [9, 11, 15-20].

The need to introduce a function of cluster size $g(L)$ distribution is dictated by the presence of clusters of different sizes in real nonequilibrium alloys. In order to take into account the function of cluster distribution by size, the profile of the main peak of the structural factor can be represented by the relation [9-10]:

$$i(s_0) = \int_0^\infty i(s_0, L)g(L)dL, \quad (5)$$

The distribution of clusters by size according to (5) takes into account scattering both on clusters and on individual atoms and can be found by taking into account the energy of cluster formation:

$$E(L,P) = A \cdot \exp\left[-\frac{U(L) + E(P)}{kT}\right], \quad (6)$$

where *U(L)* is fraction of the cluster energy associated with its size and the energy of pairwise interaction of atoms [13-14], *E(P)* is kinetic energy of the order region associated with the relative rms static displacements of atoms relative to their position in the crystalline state. To express the energy (6.7), the distribution function approaches the Gaussian distribution [9]:

$$g_G(L) = \frac{1}{\sigma_L\sqrt{2\pi}}\exp\left[-\frac{(L - \langle L\rangle)^2}{2\sigma_L^2}\right], \quad (7)$$

where

$$\sigma_L^2 = \overline{L}^2\left[\frac{\Gamma\left(\frac{3n+2}{6}\right)\Gamma\left(\frac{3n+6}{6}\right)}{\Gamma\left(\frac{3n+4}{6}\right)} - 1\right], \quad (8)$$

$\Gamma(x)$ - gamma Euler function.

Relationship (5) cannot be directly used to analyze the profile of the main peak of the structural factor, since neither the distribution parameters $g(L)$, nor the shape of the cluster areas. In this regard, the function of distribution of clusters by size is used:

$$g(L,t) = \mu \cdot \langle L\rangle \cdot e^{-\beta t^2}, \quad (9)$$

where the variables μ and β are determined by normalizing (9), and $\langle L\rangle$ is average size of the clusters.

Then (7) is transformed to the form:

$$i(s_0) = \frac{Q_2 Q_3}{d_{hkd}} \cdot \mu \cdot \langle L \rangle \cdot \exp\left(-\frac{u^2 s_0^2}{2}\right) \int_{-\infty}^{\infty} V(t) \cdot e^{-(\beta t^2 + \gamma t)} \cos(s_0 t) dt \quad (10)$$

Expression (10) is a function of the main physical parameters of the close-order amorphous system that characterizes the clusters, and the value $\langle L \rangle$ is determined in the process of modeling the profile of the main peak of the cluster structural factor. The values of the gaps (δ) between clusters in nonequilibrium alloys are not constant, however, as a first approximation, we assume them to be the same for clusters of different sizes if their shape remains constant [9]. The average size of a cluster is used to determine its average volume $\langle (L+d)^3 \rangle$ i and the average volume that falls on the same number of atoms in the volume $\langle (L+d+\delta)^3 \rangle$.

Table 1. The function of the shape *V(t)* and dimensions L of the reflection {110} of the OCC structure [14].

Cluster shape	*V(x)*	*I*	*L*	*Multiplicity*
tetrahedral bipyramid	$\mathbf{1 - \frac{3}{2}t + \frac{3}{8}t^2 + \frac{1}{8}t^3}$ 1) 2) $\mathbf{(1-t)^3}$	$\boldsymbol{I_0 - \frac{3}{2}I_1 + \frac{3}{8}I_2 + \frac{1}{8}I_3}$ $\boldsymbol{I_0 - 3I_1 + 3I_2 - I_3}$	$\mathbf{a\sqrt{2}}$ $\mathbf{a\sqrt{2}}$ $\mathbf{a\sqrt{2}}$	4 2
cuboctahedron	$\mathbf{1 - \frac{9}{5}t + \frac{4}{5}t^2}$	$\boldsymbol{I_0 - \frac{9}{5}I_1 + \frac{4}{5}I_2}$	$\mathbf{a\sqrt{2}}$	$\mathbf{a\sqrt{2}}$

Table 2. Parameters of $Cr_{88}P_{12}$ and $Fe_{88}P_{12}$, alloy clusters obtained by modeling the profile of the main peak of the structural factor.

Alloy	Main form of clusters	*a, nm*	*Δa, nm*	U^2, nm^{-2}	*δ, nm*	<L>, *nm*	Δ_L, *nm*
$Cr_{82}C_{12}$	cuboctahedron	0,28693	0,00216	0,0110	0,1510	3,4563	0,134
$Fei_{88}P_{12}$	cuboctahedron	0,28521	0,00254	0,0113	0,1321	2,5412	0,145

To determine the gaps between clusters, use the equation:

$$\frac{\langle (L+d)^3 \rangle}{\langle (L+d+\delta)^3 \rangle} = \frac{D_{\text{m/alloy}}}{D_{\text{m/cluster}}} \quad (11)$$

where $D_{\text{m/alloy}}$ is macroscopic density of the alloy, $D_{\text{m/cluster}}$ is density of the clusters, δ is average gap between clusters.

We calculate the shape function based on the Bravé principle, which states that the crystal faces with the highest reticular atomic density have the lowest surface energy. Let us consider the near-order models of the densest lattices such as the volume-centered cubic lattice, where the total number of atoms in a cluster remains constant, and the distance between parallel planes should be larger, the greater the reticular density and the interplane distances with small indices. Suppose that the growth of the cluster occurs through a series of successive states of equilibrium of the cluster with the surrounding atoms, i.e., at any given time, the surface energy of the crystal has the lowest value for a given volume (Brave-Donneuil-Harker rule) [14, 21] by virtue of the assumptions, it is possible to choose cluster shapes for the structure of a volume-centered cubic lattice bounded by planes (110), (200) or a set of these planes. Table 1 shows the shape functions *V(x)* and the peak profiles of the structural factors *i(s)* of the reflections (110) of the volume-centered cubic lattice structure.

In Table 1: a - means the length of the polyhedron edge, *L*- size of the cluster, and the length of the side edge $\mathbf{a\sqrt{\frac{3}{2}}}$ For these forms of clusters of the volume-centered cubic lattice structure, there are several orientations that lead to reflection from the {110} faces, but which have different functions *V(x)*. Table 1 shows the multiplicity of such orientations. If the multiplicity of $V_1(x)$ is 4 and, $V_2(x)$ is - 2, then

$i(s_0) = (4i_1(s_0) + 2i(s_0))/6$ due to the fact that the clusters do not have predominant orientations in the sample volume. Considering these assumptions, it is possible to calculate the profile of the main peak of the structural factor in an analytical form:

$$i(s_0) = \frac{Q_2 Q_3}{d_{hkl}} \cdot \mu \cdot \langle L \rangle \cdot \exp\left(-\frac{u^2 s_0^2}{2}\right) \cdot l, \quad (12)$$

where the values of the sub-integral expression I в in equation (12) are given in Table 1, and the values I_n are determined by Eq:

$$I_n = \left(\frac{-1}{2\beta}\right)^n \sqrt{\frac{\pi}{\beta}} \exp\left(\frac{\gamma^2 - s_0^2}{4\beta}\right)^{E\left(\frac{n}{2}\right)} \sum_{k=0} \frac{n!}{(n-2k)!\,k!} \beta^k$$
$$\sum_{\mathrm{j}=0}^{n-2k} \binom{n-2k}{\mathrm{i}} \cdot \gamma^{n-2k-j} s_0 \cdot \cos\left(\frac{s_0\gamma}{2\beta} + \frac{\pi}{2}\mathrm{j}\right)$$

where $E(n/2)$ - an integer part of a real number, $n/2$, and

$$\binom{n-2k}{i} = \frac{(n-2k)\cdot(n-2k-1)\ldots(n-2k-i+1)}{1\cdot 2\cdot 3\ldots i}, \binom{n-2k}{0} = 1$$

The modeling of the structure and average size of the clusters showed that the most realistic results are obtained when the component of the external impulse is close to one. This indicates that the clusters do not participate in translational and oscillatory motions, and one degree of freedom can be attributed to the radial momentum of the cluster, since during electrodeposition the clusters grow in the form of ellipsoids. This fact is confirmed by the analysis of the microstructure of $Cr_{88}P_{12}$ and $Fe_{88}P_{12}$ alloys (Fig. 2 - 3), which shows that during electrodeposition, the structure grows in the radial direction (under these conditions, ellipsoidal formations on the surface). The modeling of the main peak of the structural factor showed that the near-order of alloy clusters with volume-centered cubic lattice crystal lattices of the main metal have shapes close to cuboctahedra, and their sizes do not exceed 30-50 nm ((Fig. 4 - 5 and Table 2).

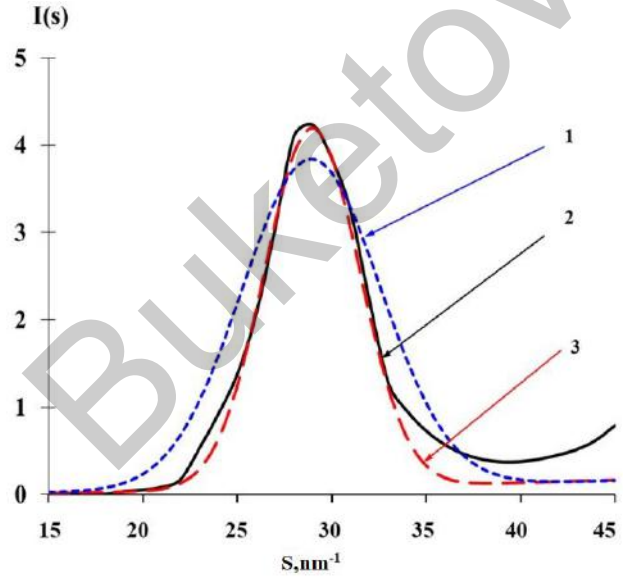

Fig. 4. Modeling the profile of the main peak of the amorphous $Cr_{88}C_{12}$ alloy:
1 - tetrahedral bipyramid, 2 - experimental peak of the structural factor, 3 - cuboctahedron

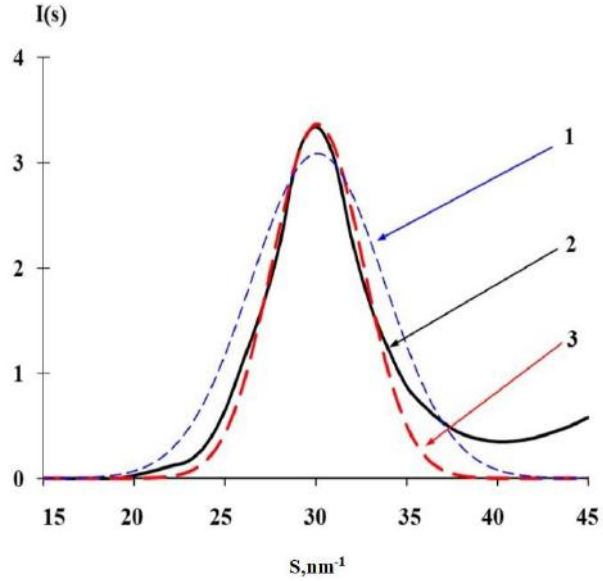

Fig. 5. Modeling of the main peak profile of the amorphous $Fe_{88}C_{12}$:
1 - tetrahedral bipyramid, 2 - experimental peak of the structural factor, 3 - cuboctahedron.

4. Conclusions

The conducted research focused on modeling the short-range order in amorphous $Cr_{88}C_{12}$ and $Fe_{88}P_{12}$ alloys has established that the most probable form of clusters in coatings based on metals with a body-centered cubic structure is the cuboctahedron. It was revealed that the shape and size distribution of $Cr_{88}C_{12}$ and $Fe_{88}P_{12}$ clusters within the surface structures are influenced by the deposition conditions, which ultimately determine the morphology of the resulting coatings. It was also determined that during the deposition process, the vector growth of clusters predominantly occurs in the radial direction, leading to the formation of ellipsoidal microstructures. Understanding the mechanisms of cluster formation opens up new opportunities for the development of advanced materials with enhanced performance and unique properties, which can be effectively utilized across various industrial sectors.

Conflict of interest statement

The authors declare that they have no conflict of interest in relation to this research, whether financial, personal, authorship or otherwise, that could affect the research and its results presented in this paper.

CRediT author statement

Sereda D.B: Conceptualization, Data Curation; **Baskevych O.S.:** Writing Original Draft; Methodology; **Kruglyak I.V.:** Investigation; **Sereda B.P.:** Supervision, Writing Review & Editing. The final manuscript was read and approved by all authors.

References

1 Danilov F.I., Protsenko V.S., Butyrina T.E., Krasinskii V.A., Baskevich A.S., Kwon S., Lee D.Y. (2011) Electrodeposition of nanocrystalline chromium coatings from Cr(III)-based electrolyte using pulse current. *Protection of Metals and Physical Chemistry of Surfaces*, 47(5), 598–605. https://doi.org/10.1134/S2070205111050066

2 Protsenko V.S., Danilov F.I., Gordienko V.O., Baskevich A.S., Artemchuk V.V. (2012) Improving hardness and tribological characteristics of nanocrystalline Cr-C films obtained from *Cr(III)* plating bath using pulsed electrodeposition. *International Journal of Refractory Metals and Hard Materials*, 35, 281–283.

3 Hu Y. C., Li F.X., Li M.Z., Bai H.Y., Wang W.H. (2015) Five-fold symmetry as an indicator of dynamic arrest in metallic glass-forming liquids. *Nature Communications,* 6, 8310. https://doi.org/10.1038/ncomms9310

4 Protsenko V. S., Bobrova L. S., Baskevich A. S., Korniy S. A., Danilov F. I. (2018) Electrodeposition of chromium coatings from a choline chloride based ionic liquid with the addition of water. *Journal of Chemical Technology and Metallurgy*, 53(5), 906–915. Available at: https://journal.uctm.edu/node/j2018-5/15_17-130_p906-915.pdf

5 Wu Z.W., et al. (2015) Hidden topological order and its correlation with glass-forming ability in metallic glasses. *Nature Communications*, 6, 6035. https://doi.org/10.1038/ncomms7035

6 Ding J., Ma E. (2017) Computational modeling sheds light on structural evolution in metallic glasses and supercooled liquids. *Computational Materials*, 3, 9. https://doi.org/10.1038/s41524-017-0007-1

7 Protsenko V. S., Bobrova L.S., Baskevich A.S., Korniy S.A., Danilov F.I. (2018) Electrodeposition of chromium coatings from a choline chloride based ionic liquid with the addition of water. *Journal of Chemical Technology and Metallurgy*, 53(5), 906–915.

8 Kuzmann E., Felner I., Sziráki L., Stichleutner S., Homonnay Z., El-Sharif M.R., Chisholm C.U. (2022) Magnetic anisotropy and microstructure in electrodeposited quaternary Sn–Fe–Ni–Co alloys with amorphous character. *Materials*, 15(9), 3015. https://doi.org/10.3390/ma15093015

9 Feng J., Chen P., Li M. (2018) Absence of 2.5 power law for fractal packing in metallic glasses. *Journal of Physics: Condensed Matter,* 30(25), 255402. https://doi.org/10.1088/1361-648X/aac45f

10 Cheng Y.Q., Ma E. (2011) Atomic-level structure and structure-property relationship in metallic glasses. *Progress in Materials Science*, 56, 379–473. https://doi.org/10.1016/j.pmatsci.2010.12.002

11 Chen D. Z., An Q., Goddard W.A., Greer J.R. (2017) Ordering and dimensional crossovers in metallic glasses and liquids. *Physical Review B,* 95(2), 024103. https://doi.org/10.1103/PhysRevB.95.024103

12 Sereda B.P., Krugliak I.V., Baskevych O.S., Belokon Y.O., Krugliak D.O., Sereda D.B. (2019) The superficial strengthening of construction materials using composition saturant environments [*Monograph*]. DDTU. 246 p. ISBN 978-966-175-187-2.

13 Chen D.Z., Wen X.D., Lu J., Wang Q.M., Wang W.H. (2015) Fractal atomic-level percolation in metallic glasses. *Science,* 349(6254), 1306–1310. https://doi.org/10.1126/science.aab1233

14 Ding J., Asta M., Ritchie R.O. (2017) On the question of fractal packing structure in metallic glasses. *Proceedings of the National Academy of Sciences,* 114(32), 8458–8463. https://doi.org/10.1073/pnas.1705723114

15 Ma D., Stoica A.D., Wang X.-L. (2009) Power-law scaling and fractal nature of medium-range order in metallic glasses. *Nature Materials*, 8(1), 30–34. https://doi.org/10.1038/nmat2340

16 Sereda B.P., Baskevych O.S., Krugliak I.V., Sereda D.B., Krugliak D.O. (2023) Obtaining protective coatings using complex functionally active charges and electrodeposition. [*Monograph*]. DDTU. 190 p. ISBN 978-966-175-244-2

17 Tang L., Wen T., Wang N., Sun Y., Zhang F., Yang Z., Ho K.-M., Wang C.-Z. (2018) Structural and chemical orders in $Ni_{64.5}Zr_{35.5}$ metallic glass by molecular dynamics simulation. *Physical Review Materials*, 2(3), 033601. https://doi.org/10.1103/PhysRevMaterials.2.033601

18 Wu Z. W., Huo C. W., Li F. X., et al. (2016). Critical scaling of icosahedral medium-range order in CuZr metallic glass-forming liquids. *Scientific Reports*, 6, 35967. https://doi.org/10.1038/srep35967

19 Zhuravel I., Mychuda L., Zhuravel Y. (2020) Localization of steel fractures based on the fractal model of their metallographic images. *Ukrainian Journal of Mechanical Engineering and Materials Science*, 6(2), 12–22. https://doi.org/10.23939/ujmems2020.02.012

20 Lu Z., Li H., Lei Z., Chang C., Wang X., Lu Z. (2018) The effects of metalloid elements on the nanocrystallization behavior and soft magnetic properties of FeCBSiPCu amorphous alloys. *Metals*, 8(4), 283. https://doi.org/10.3390/met8040283

21 Huang B., Ge T. P., Liu G. L., Luan J. (2018) Density fluctuations with fractal order in metallic glasses detected by synchrotron X-ray nano-computed tomography. *Acta Materialia, 155*, 236–244. https://doi.org/10.1016/j.actamat.2018.05.064

AUTHORS' INFORMATION

Sereda, Dmytro B. – PhD, Associate Professor, Department of Industrial Mechanical Engineering, Dnipro State Technical University, Kamenskoe, Ukraine; Scopus Author ID: 36667256600; https://orcid.org/0000-0003-4353-1365; etohardcore@gmail.com

Baskevych, Oleksandr S. – Candidate of Physical and Mathematical Sciences, Senior Researcher, Ukrainian State University of Science and Technology, Dnipro, Ukraine; Scopus Author ID: 57202232885; https:// orcid.org/0000-0002-3227-5637; abaskevich@ukr.net

Kruglyak, Irina V. – Doctor of Technical Sciences, Professor, Head of the Industrial Mechanical Engineering Department, Dnipro State Technical University, Kamenskoe, Ukraine; Scopus Author ID: 35196308100; https://orcid.org/0000-0001-8872-6778; irina6878@ukr.net

Sereda, Borys P. – Doctor of Technical Sciences, Professor, Head of the Department of Automobiles and Transportation and Logistics Systems, Dnipro State Technical University, Kamenskoe, Ukraine; Scopus Author ID: 26428911900; https://orcid.org/0000-0002-9518-381X; seredabp@ukr.net